

Measurement of the Absolute Branching Fraction for $\Lambda_c^+ \rightarrow \Lambda \mu^+ \nu_\mu$

M. Ablikim¹, M. N. Achasov^{9,e}, S. Ahmed¹⁴, X. C. Ai¹, O. Albayrak⁵, M. Albrecht⁴, D. J. Ambrose⁴⁴, A. Amoroso^{49A,49C}, F. F. An¹, Q. An^{46,a}, J. Z. Bai¹, O. Bakina²³, R. Baldini Ferroli^{20A}, Y. Ban³¹, D. W. Bennett¹⁹, J. V. Bennett⁵, N. Berger²², M. Bertani^{20A}, D. Bettoni^{21A}, J. M. Bian⁴³, F. Bianchi^{49A,49C}, E. Boger^{23,c}, I. Boyko²³, R. A. Briere⁵, H. Cai⁵¹, X. Cai^{1,a}, O. Cakir^{40A}, A. Calcaterra^{20A}, G. F. Cao¹, S. A. Cetin^{40B}, J. F. Chang^{1,a}, G. Chelkov^{23,c,d}, G. Chen¹, H. S. Chen¹, J. C. Chen¹, M. L. Chen^{1,a}, S. Chen⁴¹, S. J. Chen²⁹, X. Chen^{1,a}, X. R. Chen²⁶, Y. B. Chen^{1,a}, X. K. Chu³¹, G. Cibinetto^{21A}, H. L. Dai^{1,a}, J. P. Dai³⁴, A. Dbeyssi¹⁴, D. Dedovich²³, Z. Y. Deng¹, A. Denig²², I. Denysenko²³, M. Destefanis^{49A,49C}, F. De Mori^{49A,49C}, Y. Ding²⁷, C. Dong³⁰, J. Dong^{1,a}, L. Y. Dong¹, M. Y. Dong^{1,a}, Z. L. Dou²⁹, S. X. Du⁵³, P. F. Duan¹, J. Z. Fan³⁹, J. Fang^{1,a}, S. S. Fang¹, X. Fang^{46,a}, Y. Farinelli^{21A,21B}, L. Fava^{49B,49C}, F. Feldbauer²², G. Felici^{20A}, C. Q. Feng^{46,a}, E. Fioravanti^{21A}, M. Fritsch^{14,22}, C. D. Fu¹, Q. Gao¹, X. L. Gao^{46,a}, Y. Gao³⁹, Z. Gao^{46,a}, I. Garzia^{21A}, K. Goetzen¹⁰, L. Gong³⁰, W. X. Gong^{1,a}, W. Gradl²², M. Greco^{49A,49C}, M. H. Gu^{1,a}, Y. T. Gu¹², Y. H. Guan¹, A. Q. Guo¹, L. B. Guo²⁸, R. P. Guo¹, Y. Guo¹, Y. P. Guo²², Z. Haddadi²⁵, A. Hafner²², S. Han⁵¹, X. Q. Hao¹⁵, F. A. Harris⁴², K. L. He¹, F. H. Heinsius⁴, T. Held⁴, Y. K. Heng^{1,a}, T. Holtmann⁴, Z. L. Hou¹, C. Hu²⁸, H. M. Hu¹, J. F. Hu^{49A,49C}, T. Hu^{1,a}, Y. Hu¹, G. S. Huang^{46,a}, J. S. Huang¹⁵, X. T. Huang³³, X. Z. Huang²⁹, Z. L. Huang²⁷, T. Hussain⁴⁸, W. Ikegami Andersson⁵⁰, Q. Ji¹, Q. P. Ji¹⁵, X. B. Ji¹, X. L. Ji^{1,a}, L. W. Jiang⁵¹, X. S. Jiang^{1,a}, X. Y. Jiang³⁰, J. B. Jiao³³, Z. Jiao¹⁷, D. P. Jin^{1,a}, S. Jin¹, T. Johansson⁵⁰, A. Julin⁴³, N. Kalantar-Nayestanaki²⁵, X. L. Kang¹, X. S. Kang³⁰, M. Kavatsyuk²⁵, B. C. Ke⁵, P. Kiese²², R. Kliemt¹⁰, B. Kloss²², O. B. Kolcu^{40B,h}, B. Kopf⁴, M. Kornicer⁴², A. Kupsc⁵⁰, W. Kühn²⁴, J. S. Lange²⁴, M. Lara¹⁹, P. Larin¹⁴, L. Lavezzi^{49C,1}, H. Leithoff²², C. Leng^{49C}, C. Li⁵⁰, Cheng Li^{46,a}, D. M. Li⁵³, F. Li^{1,a}, F. Y. Li³¹, G. Li¹, H. B. Li¹, H. J. Li¹, J. C. Li¹, Jin Li³², K. Li¹³, K. Li³³, Lei Li³, P. R. Li^{7,41}, Q. Y. Li³³, T. Li³³, W. D. Li¹, W. G. Li¹, X. L. Li³³, X. N. Li^{1,a}, X. Q. Li³⁰, Y. B. Li², Z. B. Li³⁸, H. Liang^{46,a}, Y. F. Liang³⁶, Y. T. Liang²⁴, G. R. Liao¹¹, D. X. Lin¹⁴, B. Liu³⁴, B. J. Liu¹, C. X. Liu¹, D. Liu^{46,a}, F. H. Liu³⁵, Fang Liu¹, Feng Liu⁶, H. B. Liu¹², H. H. Liu¹, H. H. Liu¹⁶, H. M. Liu¹, J. Liu¹, J. B. Liu^{46,a}, J. P. Liu⁵¹, J. Y. Liu¹, K. Liu³⁹, K. Y. Liu²⁷, L. D. Liu³¹, P. L. Liu^{1,a}, Q. Liu⁴¹, Q. J. Liu³, S. B. Liu^{46,a}, X. Liu²⁶, Y. B. Liu³⁰, Y. Y. Liu³⁰, Z. A. Liu^{1,a}, Z. Q. Liu²², H. Loehner²⁵, X. C. Lou^{1,a,g}, H. J. Lu¹⁷, J. G. Lu^{1,a}, Y. Lu¹, Y. P. Lu^{1,a}, C. L. Luo²⁸, M. X. Luo⁵², T. Luo⁴², X. L. Luo^{1,a}, X. R. Lyu⁴¹, F. C. Ma²⁷, H. L. Ma¹, L. L. Ma³³, M. M. Ma¹, Q. M. Ma¹, T. Ma¹, X. N. Ma³⁰, X. Y. Ma^{1,a}, Y. M. Ma³³, F. E. Maas¹⁴, M. Maggiora^{49A,49C}, Q. A. Malik⁴⁸, Y. J. Mao³¹, Z. P. Mao¹, S. Marcello^{49A,49C}, J. G. Messchendorp²⁵, G. Mezzadri^{21B}, J. Min^{1,a}, T. J. Min¹, R. E. Mitchell¹⁹, X. H. Mo^{1,a}, Y. J. Mo⁶, C. Morales Morales¹⁴, N. Yu. Muchnoi^{9,e}, H. Muramatsu⁴³, P. Musiol⁴, Y. Nefedov²³, F. Nerling¹⁰, I. B. Nikolaev^{9,e}, Z. Ning^{1,a}, S. Nisar⁸, S. L. Niu^{1,a}, X. Y. Niu¹, S. L. Olsen³², Q. Ouyang^{1,a}, S. Pacetti^{20B}, Y. Pan^{46,a}, P. Patteri^{20A}, M. Pelizaeus⁴, H. P. Peng^{46,a}, K. Peters^{10,i}, J. Pettersson⁵⁰, J. L. Ping²⁸, R. G. Ping¹, R. Poling⁴³, V. Prasad¹, H. R. Qi², M. Qi²⁹, S. Qian^{1,a}, C. F. Qiao⁴¹, L. Q. Qin³³, N. Qin⁵¹, X. S. Qin¹, Z. H. Qin^{1,a}, J. F. Qiu¹, K. H. Rashid⁴⁸, C. F. Redmer²², M. Ripka²², G. Rong¹, Ch. Rosner¹⁴, X. D. Ruan¹², A. Sarantsev^{23,f}, M. Savrié^{21B}, C. Schnier⁴, K. Schoenning⁵⁰, W. Shan³¹, M. Shao^{46,a}, C. P. Shen², P. X. Shen³⁰, X. Y. Shen¹, H. Y. Sheng¹, W. M. Song¹, X. Y. Song¹, S. Sosio^{49A,49C}, S. Spataro^{49A,49C}, G. X. Sun¹, J. F. Sun¹⁵, S. S. Sun¹, X. H. Sun¹, Y. J. Sun^{46,a}, Y. Z. Sun¹, Z. J. Sun^{1,a}, Z. T. Sun¹⁹, C. J. Tang³⁶, X. Tang¹, I. Tapan^{40C}, E. H. Thorndike⁴⁴, M. Tiemens²⁵, I. Uman^{40D}, G. S. Varner⁴², B. Wang³⁰, B. L. Wang⁴¹, D. Wang³¹, D. Y. Wang³¹, K. Wang^{1,a}, L. L. Wang¹, L. S. Wang¹, M. Wang³³, P. Wang¹, P. L. Wang¹, W. Wang^{1,a}, W. P. Wang^{46,a}, X. F. Wang³⁹, Y. Wang³⁷, Y. D. Wang¹⁴, Y. F. Wang^{1,a}, Y. Q. Wang²², Z. Wang^{1,a}, Z. G. Wang^{1,a}, Z. H. Wang^{46,a}, Z. Y. Wang¹, T. Weber²², D. H. Wei¹¹, P. Weidenkaff²², S. P. Wen¹, U. Wiedner⁴, M. Wolke⁵⁰, L. H. Wu¹, L. J. Wu¹, Z. Wu^{1,a}, L. Xia^{46,a}, L. G. Xia³⁹, Y. Xia¹⁸, D. Xiao¹, H. Xiao⁴⁷, Z. J. Xiao²⁸, Y. G. Xie^{1,a}, Yuehong Xie⁶, Q. L. Xiu^{1,a}, G. F. Xu¹, J. J. Xu¹, L. Xu¹, Q. J. Xu¹³, Q. N. Xu⁴¹, X. P. Xu³⁷, L. Yan^{49A,49C}, W. B. Yan^{46,a}, W. C. Yan^{46,a}, Y. H. Yan¹⁸, H. J. Yang^{34,j}, H. X. Yang¹, L. Yang⁵¹, Y. X. Yang¹¹, M. Ye^{1,a}, M. H. Ye⁷, J. H. Yin¹, Z. Y. You³⁸, B. X. Yu^{1,a}, C. X. Yu³⁰, J. S. Yu²⁶, C. Z. Yuan¹, Y. Yuan¹, A. Yuncu^{40B,b}, A. A. Zafar⁴⁸, Y. Zeng¹⁸, Z. Zeng^{46,a}, B. X. Zhang¹, B. Y. Zhang^{1,a}, C. C. Zhang¹, D. H. Zhang¹, H. H. Zhang³⁸, H. Y. Zhang^{1,a}, J. Zhang¹, J. J. Zhang¹, J. L. Zhang¹, J. Q. Zhang¹, J. W. Zhang^{1,a}, J. Y. Zhang¹, J. Z. Zhang¹, K. Zhang¹, L. Zhang¹, S. Q. Zhang³⁰, X. Y. Zhang³³, Y. Zhang¹, Y. H. Zhang⁴¹, Y. N. Zhang⁴¹, Y. T. Zhang^{46,a}, Yu Zhang⁴¹, Z. H. Zhang⁶, Z. P. Zhang⁴⁶, Z. Y. Zhang⁵¹, G. Zhao¹, J. W. Zhao^{1,a}, J. Y. Zhao¹, J. Z. Zhao^{1,a}, Lei Zhao^{46,a}, Ling Zhao¹, M. G. Zhao³⁰, Q. Zhao¹, Q. W. Zhao¹, S. J. Zhao⁵³, T. C. Zhao¹, Y. B. Zhao^{1,a}, Z. G. Zhao^{46,a}, A. Zhemchugov^{23,c}, B. Zheng⁴⁷, J. P. Zheng^{1,a}, W. J. Zheng³³, Y. H. Zheng⁴¹, B. Zhong²⁸, L. Zhou^{1,a}, X. Zhou⁵¹, X. K. Zhou^{46,a}, X. R. Zhou^{46,a}, X. Y. Zhou¹, K. Zhu¹, K. J. Zhu^{1,a}, S. Zhu¹, S. H. Zhu⁴⁵, X. L. Zhu³⁹, Y. C. Zhu^{46,a}, Y. S. Zhu¹, Z. A. Zhu¹, J. Zhuang^{1,a}, L. Zotti^{49A,49C}, B. S. Zou¹, J. H. Zou¹

(BESIII Collaboration)

¹ Institute of High Energy Physics, Beijing 100049, People's Republic of China

² Beihang University, Beijing 100191, People's Republic of China

³ Beijing Institute of Petrochemical Technology, Beijing 102617, People's Republic of China

⁴ Bochum Ruhr-University, D-44780 Bochum, Germany

- ⁵ Carnegie Mellon University, Pittsburgh, Pennsylvania 15213, USA
- ⁶ Central China Normal University, Wuhan 430079, People's Republic of China
- ⁷ China Center of Advanced Science and Technology, Beijing 100190, People's Republic of China
- ⁸ COMSATS Institute of Information Technology, Lahore, Defence Road, Off Raiwind Road, 54000 Lahore, Pakistan
- ⁹ G.I. Budker Institute of Nuclear Physics SB RAS (BINP), Novosibirsk 630090, Russia
- ¹⁰ GSI Helmholtzcentre for Heavy Ion Research GmbH, D-64291 Darmstadt, Germany
- ¹¹ Guangxi Normal University, Guilin 541004, People's Republic of China
- ¹² Guangxi University, Nanning 530004, People's Republic of China
- ¹³ Hangzhou Normal University, Hangzhou 310036, People's Republic of China
- ¹⁴ Helmholtz Institute Mainz, Johann-Joachim-Becher-Weg 45, D-55099 Mainz, Germany
- ¹⁵ Henan Normal University, Xinxiang 453007, People's Republic of China
- ¹⁶ Henan University of Science and Technology, Luoyang 471003, People's Republic of China
- ¹⁷ Huangshan College, Huangshan 245000, People's Republic of China
- ¹⁸ Hunan University, Changsha 410082, People's Republic of China
- ¹⁹ Indiana University, Bloomington, Indiana 47405, USA
- ²⁰ (A)INFN Laboratori Nazionali di Frascati, I-00044, Frascati, Italy; (B)INFN and University of Perugia, I-06100, Perugia, Italy
- ²¹ (A)INFN Sezione di Ferrara, I-44122, Ferrara, Italy; (B)University of Ferrara, I-44122, Ferrara, Italy
- ²² Johannes Gutenberg University of Mainz, Johann-Joachim-Becher-Weg 45, D-55099 Mainz, Germany
- ²³ Joint Institute for Nuclear Research, 141980 Dubna, Moscow region, Russia
- ²⁴ Justus-Liebig-Universitaet Giessen, II. Physikalisches Institut, Heinrich-Buff-Ring 16, D-35392 Giessen, Germany
- ²⁵ KVI-CART, University of Groningen, NL-9747 AA Groningen, The Netherlands
- ²⁶ Lanzhou University, Lanzhou 730000, People's Republic of China
- ²⁷ Liaoning University, Shenyang 110036, People's Republic of China
- ²⁸ Nanjing Normal University, Nanjing 210023, People's Republic of China
- ²⁹ Nanjing University, Nanjing 210093, People's Republic of China
- ³⁰ Nankai University, Tianjin 300071, People's Republic of China
- ³¹ Peking University, Beijing 100871, People's Republic of China
- ³² Seoul National University, Seoul, 151-747 Korea
- ³³ Shandong University, Jinan 250100, People's Republic of China
- ³⁴ Shanghai Jiao Tong University, Shanghai 200240, People's Republic of China
- ³⁵ Shanxi University, Taiyuan 030006, People's Republic of China
- ³⁶ Sichuan University, Chengdu 610064, People's Republic of China
- ³⁷ Soochow University, Suzhou 215006, People's Republic of China
- ³⁸ Sun Yat-Sen University, Guangzhou 510275, People's Republic of China
- ³⁹ Tsinghua University, Beijing 100084, People's Republic of China
- ⁴⁰ (A)Ankara University, 06100 Tandogan, Ankara, Turkey; (B)Istanbul Bilgi University, 34060 Eyup, Istanbul, Turkey; (C)Uludag University, 16059 Bursa, Turkey; (D)Near East University, Nicosia, North Cyprus, Mersin 10, Turkey
- ⁴¹ University of Chinese Academy of Sciences, Beijing 100049, People's Republic of China
- ⁴² University of Hawaii, Honolulu, Hawaii 96822, USA
- ⁴³ University of Minnesota, Minneapolis, Minnesota 55455, USA
- ⁴⁴ University of Rochester, Rochester, New York 14627, USA
- ⁴⁵ University of Science and Technology Liaoning, Anshan 114051, People's Republic of China
- ⁴⁶ University of Science and Technology of China, Hefei 230026, People's Republic of China
- ⁴⁷ University of South China, Hengyang 421001, People's Republic of China
- ⁴⁸ University of the Punjab, Lahore-54590, Pakistan
- ⁴⁹ (A)University of Turin, I-10125, Turin, Italy; (B)University of Eastern Piedmont, I-15121, Alessandria, Italy; (C)INFN, I-10125, Turin, Italy
- ⁵⁰ Uppsala University, Box 516, SE-75120 Uppsala, Sweden
- ⁵¹ Wuhan University, Wuhan 430072, People's Republic of China
- ⁵² Zhejiang University, Hangzhou 310027, People's Republic of China
- ⁵³ Zhengzhou University, Zhengzhou 450001, People's Republic of China
- ^a Also at State Key Laboratory of Particle Detection and Electronics, Beijing 100049, Hefei 230026, People's Republic of China
- ^b Also at Bogazici University, 34342 Istanbul, Turkey
- ^c Also at the Moscow Institute of Physics and Technology, Moscow 141700, Russia
- ^d Also at the Functional Electronics Laboratory, Tomsk State University, Tomsk, 634050, Russia
- ^e Also at the Novosibirsk State University, Novosibirsk, 630090, Russia

^f Also at the NRC “Kurchatov Institute”, PNPI, 188300, Gatchina, Russia

^g Also at University of Texas at Dallas, Richardson, Texas 75083, USA

^h Also at Istanbul Arel University, 34295 Istanbul, Turkey

ⁱ Also at Goethe University Frankfurt, 60323 Frankfurt am Main, Germany

^j Also at Institute of Nuclear and Particle Physics, Shanghai Key Laboratory for Particle Physics and Cosmology, Shanghai 200240, People’s Republic of China

Abstract

We report the first measurement of the absolute branching fraction for $\Lambda_c^+ \rightarrow \Lambda\mu^+\nu_\mu$. This measurement is based on a sample of e^+e^- annihilation data at a center-of-mass energy of $\sqrt{s} = 4.6$ GeV collected with the BESIII detector at the BEPCII storage rings. The sample corresponds to an integrated luminosity of 567 pb^{-1} . The branching fraction is determined to be $\mathcal{B}(\Lambda_c^+ \rightarrow \Lambda\mu^+\nu_\mu) = (3.49 \pm 0.46(\text{stat}) \pm 0.27(\text{syst}))\%$. In addition, we calculate the ratio $\mathcal{B}(\Lambda_c^+ \rightarrow \Lambda\mu^+\nu_\mu)/\mathcal{B}(\Lambda_c^+ \rightarrow \Lambda e^+\nu_e)$ to be $0.96 \pm 0.16(\text{stat}) \pm 0.04(\text{syst})$.

Keywords: Λ_c^+ , semi-leptonic decay, absolute branching fraction, BESIII

1. Introduction

Semileptonic (SL) decays of the lightest charmed baryon, Λ_c^+ , provide a stringent test for non-perturbative aspects of the strong interaction theory. The $\Lambda_c^+ \rightarrow \Lambda\ell^+\nu_\ell$ (ℓ denotes lepton) decay is dominated by the Cabibbo-favored transition $c \rightarrow s\ell^+\nu_\ell$, which occurs independently of the spin-zero and isospin-zero spectator ud diquark, to good approximation. This leads to a simpler theoretical description and greater predictive power in the non-perturbative models than in the case for charmed mesons [1]. Predictions of the branching fraction (BF) $\mathcal{B}(\Lambda_c^+ \rightarrow \Lambda\ell^+\nu_\ell)$ in different theoretical models vary over a wide range from 1.4% to 9.2% [2, 3, 4, 5, 6, 7, 8, 9, 10, 11, 12, 13], depending on the choice of Λ_c^+ wave function model and the treatment of decay dynamics. In 2015, BESIII measured the absolute BF for $\Lambda_c^+ \rightarrow \Lambda e^+\nu_e$ to be $\mathcal{B}(\Lambda_c^+ \rightarrow \Lambda e^+\nu_e) = (3.63 \pm 0.38 \pm 0.20)\%$ [14], which disfavors the predictions in Refs. [2, 3, 5, 6, 7] at the 95% confidence level. It is desirable to test these theoretical predictions by measuring $\mathcal{B}(\Lambda_c^+ \rightarrow \Lambda\mu^+\nu_\mu)$. In addition, lepton universality can be tested by comparing the BFs between the electronic and muonic modes.

In this paper, we report the first absolute measurement of $\mathcal{B}(\Lambda_c^+ \rightarrow \Lambda\mu^+\nu_\mu)$ by analyzing a data sample with an integrated luminosity of 567 pb^{-1} [15] accumulated at a center-of-mass (c.m.) energy of $\sqrt{s} = 4.6$ GeV with the BESIII detector at the BEPCII col-

lider, which is the largest e^+e^- collision sample near the $\Lambda_c^+\bar{\Lambda}_c^-$ mass threshold. At this energy, the Λ_c^+ is produced in company with one $\bar{\Lambda}_c^-$ baryon only, and no other hadrons are kinematically allowed. Hence, $\mathcal{B}(\Lambda_c^+ \rightarrow \Lambda\mu^+\nu_\mu)$ can be accessed by measuring the relative probability of finding the SL decay when the $\bar{\Lambda}_c^-$ is detected in a number of prolific decay channels. This will provide a straightforward and direct BF measurement without requiring knowledge of the total number of $\Lambda_c^+\bar{\Lambda}_c^-$ pairs produced. In the following, charge conjugated modes are always implied, unless explicitly mentioned.

2. BESIII Detector and Monte Carlo Simulation

The BESIII [16] detector is a cylindrical detector with a solid-angle coverage of 93% of 4π that operates at the BEPCII collider. It consists of a Helium-gas based main drift chamber (MDC), a plastic scintillator time-of-flight (TOF) system, a CsI (Tl) electromagnetic calorimeter (EMC), a superconducting solenoid providing a 1.0 T magnetic field and a muon counter. The charged particle momentum resolution is 0.5% at a transverse momentum of 1 GeV/c. The photon energy resolution in the EMC is 2.5% in the barrel and 5.0% in the end-caps at 1 GeV. More details about the design and performance of the detector are given in Ref. [16].

A GEANT4-based [17] Monte Carlo (MC) simulation package, which includes the geometric descrip-

tion of the detector and the detector response, is used to determine the detection efficiency and to estimate the potential backgrounds. Signal MC samples of a Λ_c^+ baryon decaying only to $\Lambda\mu^+\nu_\mu$ together with a $\bar{\Lambda}_c^-$ decaying to specified modes are generated with the KKMC [18] and EVTGEN [19], taking into account the initial state radiation (ISR) [20] and the final state radiation (FSR) [21] effects. For the simulation of the process $\Lambda_c^+ \rightarrow \Lambda\mu^+\nu_\mu$, we use the form factor obtained using Heavy Quark Effective Theory and QCD sum rules in Ref. [10]. To study backgrounds, inclusive MC samples are simulated which consist of $\Lambda_c^+\bar{\Lambda}_c^-$ events, $D_{(s)}^*\bar{D}_{(s)}^{(*)} + X$ production, ISR return to the charmonium(-like) ψ states at lower masses, and QED processes. The decay modes with known BF's of the Λ_c , ψ and $D_{(s)}$ particles taken from Particle Data Group (PDG) [22] are simulated with EVTGEN, while the remaining unknown decays are generated with LUNDCHARM [23].

3. Analysis

Following the similar technique of the single tag (ST) and double tag (DT) in Ref. [14], we reconstruct the $\bar{\Lambda}_c^-$ baryons in eleven hadronic decay modes as listed in the first column of Table 1. The intermediate particles K_S^0 , $\bar{\Lambda}$, $\bar{\Sigma}^0$, $\bar{\Sigma}^-$ and π^0 are reconstructed through their decays $K_S^0 \rightarrow \pi^+\pi^-$, $\bar{\Lambda} \rightarrow \bar{p}\pi^+$, $\bar{\Sigma}^0 \rightarrow \gamma\bar{\Lambda}$ with $\bar{\Lambda} \rightarrow \bar{p}\pi^+$, $\bar{\Sigma}^- \rightarrow \bar{p}\pi^0$ and $\pi^0 \rightarrow \gamma\gamma$, respectively. The detailed selection criteria for charged and neutral tracks, π^0 , K_S^0 and $\bar{\Lambda}$ candidates used in the reconstruction of tags are described in Ref. [14].

In this analysis, the ST $\bar{\Lambda}_c^-$ signals are identified using the beam energy constrained mass, $M_{BC} = \sqrt{E_{\text{beam}}^2/c^4 - |\vec{p}_{\bar{\Lambda}_c^-}|^2/c^2}$, where E_{beam} is the beam energy and $\vec{p}_{\bar{\Lambda}_c^-}$ is the momentum of the $\bar{\Lambda}_c^-$ candidate. To improve the signal purity, the energy difference $\Delta E = E_{\text{beam}} - E_{\bar{\Lambda}_c^-}$ for each candidate is required to be within $\pm 3\sigma_{\Delta E}$ around the ΔE peak, where $\sigma_{\Delta E}$ is the ΔE resolution and $E_{\bar{\Lambda}_c^-}$ is the reconstructed $\bar{\Lambda}_c^-$ energy. Table 1 shows the mode dependent ΔE requirements and the ST yields in the M_{BC} signal region (2.280, 2.296) GeV/ c^2 , which are obtained by a fit to the M_{BC} distributions. The detailed process to extract the ST signal yields is described in Ref. [14]. The total ST yield summed over all 11 modes is $N_{\bar{\Lambda}_c^-}^{\text{tot}} = 14415 \pm 159$, where the uncertainty is statistical only.

Candidate events for $\Lambda_c^+ \rightarrow \Lambda\mu^+\nu_\mu$ are selected from the remaining tracks recoiling against the ST $\bar{\Lambda}_c^-$ candidates. The Λ candidate is formed from a $p\pi^-$ combination that is constrained by a common vertex fit to

have a positive decay length L . If multiple Λ candidates are formed, the one with the largest L/σ_L is retained, where σ_L is the resolution of the measured L . Particle identification (PID) is performed using probabilities derived from the specific energy loss dE/dx measured by the MDC, the time of flight measured by the TOF, and energy measured by the EMC; a μ candidate is required to satisfy $\mathcal{L}'_\mu > 0.001$, $\mathcal{L}'_\mu > \mathcal{L}'_e$ and $\mathcal{L}'_\mu > \mathcal{L}'_K$, where \mathcal{L}'_μ , \mathcal{L}'_e , and \mathcal{L}'_K are the probabilities for a muon, electron, and kaon, respectively.

Studies on the inclusive MC samples show that the backgrounds are dominated by $\Lambda_c^+ \rightarrow \Lambda\pi^+$, $\Sigma^0\pi^+$ and $\Lambda\pi^+\pi^0$. Backgrounds from $\Lambda_c^+ \rightarrow \Lambda\pi^+$ and $\Lambda_c^+ \rightarrow \Sigma^0\pi^+$ are rejected by requiring the $\Lambda\mu^+$ invariant mass $M_{\Lambda\mu^+}$ is less than 2.12 GeV/ c^2 . The background from $\Lambda_c^+ \rightarrow \Lambda\pi^+\pi^0$ is suppressed by requiring the largest energy of any unused photons $E_{\gamma_{\text{max}}}$ be less than 0.25 GeV and the deposited energy for the muon candidate in the EMC be less than 0.30 GeV.

Since the neutrino is not detected, we employ the kinematic variable $U_{\text{miss}} \equiv E_{\text{miss}} - |\vec{p}_{\text{miss}} c|$ to identify the neutrino signal, where E_{miss} and \vec{p}_{miss} are the missing energy and momentum carried by the neutrino, respectively. They are calculated as $E_{\text{miss}} = E_{\text{beam}} - E_\Lambda - E_{\mu^+}$ and $\vec{p}_{\text{miss}} = \vec{p}_{\Lambda_c^+} - \vec{p}_\Lambda - \vec{p}_{\mu^+}$, where $\vec{p}_{\Lambda_c^+}$ is the momentum of the Λ_c^+ baryon, $E_\Lambda(\vec{p}_\Lambda)$ and $E_{\mu^+}(\vec{p}_{\mu^+})$ are the energies (momenta) of the Λ and μ^+ , respectively. Here, the momentum $\vec{p}_{\Lambda_c^+}$ is given by $\vec{p}_{\Lambda_c^+} = -\hat{p}_{\text{tag}} \sqrt{E_{\text{beam}}^2/c^2 - m_{\bar{\Lambda}_c^-}^2}$, where \hat{p}_{tag} is the momentum direction of the ST $\bar{\Lambda}_c^-$ and $m_{\bar{\Lambda}_c^-}$ is the nominal $\bar{\Lambda}_c^-$ mass [22]. For the signal events, the U_{miss} distribution is expected to peak at zero.

The distribution of the $p\pi^-$ invariant mass $M_{p\pi^-}$ versus U_{miss} for the $\Lambda_c^+ \rightarrow \Lambda\mu^+\nu_\mu$ candidates in data is shown in Fig. 1 (a), where a cluster around the signal region is evident. After requiring $M_{p\pi^-}$ to be within the Λ signal region, the projection of U_{miss} is shown in Fig. 1(b). Two bumps, which correspond to the signal peak (left side) and background $\Lambda_c^+ \rightarrow \Lambda\pi^+\pi^0$ (right side), are visible. According to MC simulations, the survival rate of the background process $\Lambda_c^+ \rightarrow \Lambda\pi^+\pi^0$ is estimated to be $\eta_{\Lambda\pi^+\pi^0} = (3.67 \pm 0.05)\%$, where the BF's for $\Lambda \rightarrow p\pi^-$ and $\pi^0 \rightarrow \gamma\gamma$ are included. Thus, the number of the $\Lambda_c^+ \rightarrow \Lambda\pi^+\pi^0$ background events can be estimated by

$$N_{\Lambda\pi^+\pi^0}^{\text{bkg}} = N_{\bar{\Lambda}_c^-}^{\text{tot}} \cdot \mathcal{B}(\Lambda_c^+ \rightarrow \Lambda\pi^+\pi^0) \cdot \eta_{\Lambda\pi^+\pi^0}. \quad (1)$$

Inserting the values of $N_{\bar{\Lambda}_c^-}^{\text{tot}}$, $\eta_{\Lambda\pi^+\pi^0}$ and $\mathcal{B}(\Lambda_c^+ \rightarrow \Lambda\pi^+\pi^0) = (7.01 \pm 0.42)\%$ [24] in Eq. (1), we obtain $N_{\Lambda\pi^+\pi^0}^{\text{bkg}} = 37.1 \pm 2.3$, where the uncertainties from

TABLE 1: ΔE requirements and ST yields $N_{\bar{\Lambda}_c^-}$ in data, in which the uncertainties are statistical only.

Mode	ΔE (GeV)	$N_{\bar{\Lambda}_c^-}$
$\bar{p}K_S^0$	$[-0.025, 0.028]$	1066 ± 33
$\bar{p}K^+\pi^-$	$[-0.019, 0.023]$	5692 ± 88
$\bar{p}K_S^0\pi^0$	$[-0.035, 0.049]$	593 ± 41
$\bar{p}K^+\pi^-\pi^0$	$[-0.044, 0.052]$	1547 ± 61
$\bar{p}K_S^0\pi^+\pi^-$	$[-0.029, 0.032]$	516 ± 34
$\bar{\Lambda}\pi^-$	$[-0.033, 0.035]$	593 ± 25
$\bar{\Lambda}\pi^-\pi^0$	$[-0.037, 0.052]$	1864 ± 56
$\bar{\Lambda}\pi^-\pi^+\pi^-$	$[-0.028, 0.030]$	674 ± 36
$\bar{\Sigma}^0\pi^-$	$[-0.029, 0.032]$	532 ± 30
$\bar{\Sigma}^-\pi^0$	$[-0.038, 0.062]$	329 ± 28
$\bar{\Sigma}^-\pi^+\pi^-$	$[-0.049, 0.054]$	1009 ± 57

$N_{\bar{\Lambda}_c^-}^{\text{tot}}$, $\eta_{\Lambda\pi^+\pi^0}$ and $\mathcal{B}(\Lambda_c^+ \rightarrow \Lambda\pi^+\pi^0)$ are included.

We apply a fit to the U_{miss} distribution to obtain the signal yields. The $\Lambda_c^+ \rightarrow \Lambda\mu^+\nu_\mu$ signal shape is described with a function f , which consists of a Gaussian function to model the core of the U_{miss} distribution and two power law tails to account for the effects of ISR and FSR in the form [25] of

$$f(U_{\text{miss}}) = \begin{cases} p_1 \left(\frac{n_1}{\alpha_1} - \alpha_1 + t \right)^{-n_1}, & t > \alpha_1 \\ e^{-t^2/2}, & -\alpha_2 < t < \alpha_1 \\ p_2 \left(\frac{n_2}{\alpha_2} - \alpha_2 - t \right)^{-n_2}, & t < -\alpha_2 \end{cases} \quad (2)$$

Here, $t \equiv (U_{\text{miss}} - U_{\text{mean}})/\sigma_{U_{\text{miss}}}$, U_{mean} and $\sigma_{U_{\text{miss}}}$ are the mean value and resolution of the Gaussian function, respectively, $p_1 \equiv (n_1/\alpha_1)^{n_1} e^{-\alpha_1^2/2}$ and $p_2 \equiv (n_2/\alpha_2)^{n_2} e^{-\alpha_2^2/2}$. The parameters α_1 , α_2 , n_1 and n_2 are fixed to the values obtained by studying the signal MC simulations. For backgrounds, a double Gaussian function with parameters fixed according to MC simulations is used to describe the $\Lambda_c^+ \rightarrow \Lambda\pi^+\pi^0$ peaking background and a MC-derived shape is used to describe other combinatorial backgrounds. In the fit, we fix the number of the $\Lambda_c^+ \rightarrow \Lambda\pi^+\pi^0$ background events to be estimated $N_{\Lambda\pi^+\pi^0}^{\text{bkg}}$ as described above. From the fit, we obtain the number of events of $\Lambda_c^+ \rightarrow \Lambda\mu^+\nu_\mu$ to be $N_{\Lambda\mu^+\nu_\mu}^{\text{obs}} = 78.7 \pm 10.5$, where the uncertainty is statistical only. A fit with unconstrained $N_{\Lambda\pi^+\pi^0}^{\text{bkg}}$ gives 77.1 ± 11.4 events of signal, which is in good agreement with the estimation when $N_{\Lambda\pi^+\pi^0}^{\text{bkg}}$ is fixed. Based on the data in Λ sidebands in Fig. 1(a), the background events from the non- Λ SL decays is found to be negligible.

The absolute BF for $\Lambda_c^+ \rightarrow \Lambda\mu^+\nu_\mu$ is determined

with

$$\mathcal{B}(\Lambda_c^+ \rightarrow \Lambda\mu^+\nu_\mu) = \frac{N_{\Lambda\mu^+\nu_\mu}^{\text{obs}}}{N_{\bar{\Lambda}_c^-}^{\text{tot}} \cdot \varepsilon_{\Lambda\mu^+\nu_\mu} \cdot \mathcal{B}(\Lambda \rightarrow p\pi^-)}, \quad (3)$$

where $\varepsilon_{\Lambda\mu^+\nu_\mu}$ is the detection efficiency for the $\Lambda_c^+ \rightarrow \Lambda\mu^+\nu_\mu$ decay, which does not include the BF for $\Lambda \rightarrow p\pi^-$. For each ST mode i , the efficiency $\varepsilon_{\Lambda\mu^+\nu_\mu}^i$ is obtained by dividing the DT efficiency $\varepsilon_{\text{tag}, \Lambda\mu^+\nu_\mu}^i$ by the ST efficiency $\varepsilon_{\text{tag}}^i$. After weighting $\varepsilon_{\Lambda\mu^+\nu_\mu}^i$ with the ST yields in data for each ST mode i , we determine the overall average efficiency $\varepsilon_{\Lambda\mu^+\nu_\mu} = (24.5 \pm 0.2)\%$. By inserting the values of $N_{\Lambda\mu^+\nu_\mu}^{\text{obs}}$, $N_{\bar{\Lambda}_c^-}^{\text{tot}}$, $\varepsilon_{\Lambda\mu^+\nu_\mu}$ and $\mathcal{B}(\Lambda \rightarrow p\pi^-)$ [22] in Eq. (3), we obtain $\mathcal{B}(\Lambda_c^+ \rightarrow \Lambda\mu^+\nu_\mu) = (3.49 \pm 0.46 \pm 0.27)\%$, where the first uncertainty is statistical, and the second uncertainty is systematic as described below.

With the DT technique, the uncertainties on the BF measurement are insensitive to those originating from the ST side. The systematic uncertainties for measuring $\mathcal{B}(\Lambda_c^+ \rightarrow \Lambda\mu^+\nu_\mu)$ mainly arise from the uncertainties related to the tracking and PID of the muon candidate, Λ reconstruction, U_{miss} fit, peaking background subtraction, $E_{\gamma\text{max}}$ and $M_{\Lambda\mu^+}$ requirements, and signal MC modeling. Throughout this paragraph, the systematic uncertainties quoted are relative uncertainties. The uncertainties of the μ^+ tracking and PID are determined to be 1.0% and 2.0%, respectively, by studying a control sample of $e^+e^- \rightarrow (\gamma)\mu^+\mu^-$ events. The uncertainty of the Λ reconstruction is determined to be 2.5% by studying a control sample of $\chi_{cJ} \rightarrow \Lambda\bar{\Lambda}\pi^+\pi^-$ decays. The uncertainty of U_{miss} fit is estimated to be 1.5% obtained by varying the fitting range and examining the fluctuation of the non-peaking background shape. The uncertainty due to peaking background

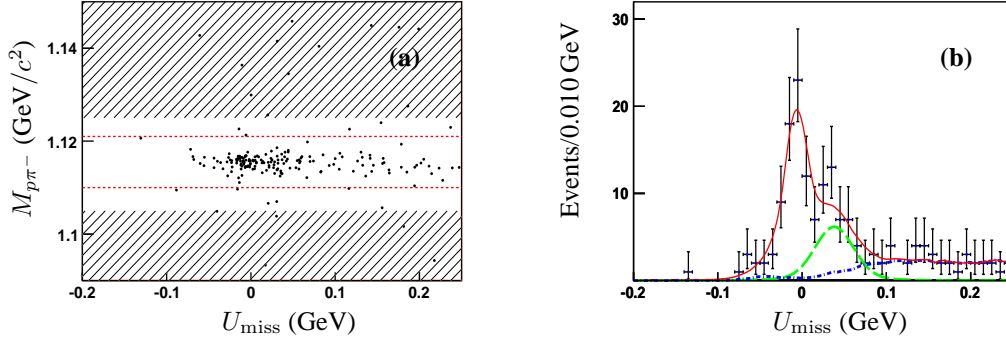


FIG. 1: (a) Distribution of $M_{p\pi^-}$ versus U_{miss} for the $\Lambda_c^+ \rightarrow \Lambda\mu^+\nu_\mu$ candidates in data. The area between the dashed lines denotes the Λ signal region and the hatched areas indicate the Λ sideband regions. (b) Fit to the U_{miss} distribution within the Λ signal region. Data are shown as the dots with error bars. The long-dashed curve (green) shows the $\Lambda_c^+ \rightarrow \Lambda\pi^+\pi^0$ background while the dot-dashed curve (blue) shows other Λ_c^+ decay backgrounds. The thick line (red) shows the total fit.

$\Lambda_c^+ \rightarrow \Lambda\pi^+\pi^0$ subtraction is estimated to be 2.5% obtained by varying $N_{\Lambda\pi^+\pi^0}^{\text{bkg}}$ equivalent variations of $\pm 1\sigma$ of the quoted BF, and smearing the MC-derived shape of $\Lambda_c^+ \rightarrow \Lambda\pi^+\pi^0$ backgrounds with a Gaussian function to accommodate the resolution difference between the data and MC simulation. The uncertainty in the $E_{\gamma\text{max}}$ requirement is estimated to be 2.6% by using a control sample of $e^+e^- \rightarrow p\bar{p}\pi^+\pi^-$ events. The uncertainty in the $M_{\Lambda\mu^+}$ requirement is estimated to be 2.0% by comparing the obtained $\mathcal{B}(\Lambda_c^+ \rightarrow \Lambda\mu^+\nu_\mu)$ under the alternative requirements of $M_{\Lambda\mu^+} < 2.07 \text{ GeV}/c^2$ or $M_{\Lambda\mu^+} < 2.17 \text{ GeV}/c^2$ with the nominal value. The uncertainty in the signal MC model is estimated to be 5.2% by varying the parameterization of the form factor function according to Refs. [10, 26] and by taking into account the q^2 dependence observed in data. In addition, there are systematic uncertainties from the quoted $\mathcal{B}(\Lambda \rightarrow p\pi^-)$ (0.8%), the $N_{\Lambda_c^-}^{\text{tot}}$ (1.0%) evaluated by using alternative signal shapes in the fits to the M_{BC} spectra [14], and MC statistics (0.8%). All these systematic uncertainties are summarized in Table 2, and the total systematic uncertainty is evaluated to be 7.7% by summing up all the individual contributions in quadrature.

The ratio of branching fractions $\mathcal{B}(\Lambda_c^+ \rightarrow \Lambda\mu^+\nu_\mu)/\mathcal{B}(\Lambda_c^+ \rightarrow \Lambda e^+\nu_e)$ is calculated with the measured $\mathcal{B}(\Lambda_c^+ \rightarrow \Lambda\mu^+\nu_\mu)$ in this work and $\mathcal{B}(\Lambda_c^+ \rightarrow \Lambda e^+\nu_e) = (3.63 \pm 0.38(\text{stat}) \pm 0.20(\text{syst}))\%$ from BESIII [14]. We determine $\mathcal{B}(\Lambda_c^+ \rightarrow \Lambda\mu^+\nu_\mu)/\mathcal{B}(\Lambda_c^+ \rightarrow \Lambda e^+\nu_e)$ to be $0.96 \pm 0.16 \pm 0.04$, where the first uncertainty is statistical and the second is systematic, in which the common systematic uncertainties from the tracking efficiency, the Λ reconstruction, the quoted BF for $\Lambda \rightarrow p\pi^-$, the number of Λ_c^- tags $N_{\Lambda_c^-}^{\text{tot}}$ and the MC model cancel.

4. Summary

In summary, based on the e^+e^- collision data corresponding to an integrated luminosity of 567 pb^{-1} taken at $\sqrt{s} = 4.6 \text{ GeV}$ with the BESIII detector, we report the first direct measurement of the absolute BF for $\Lambda_c^+ \rightarrow \Lambda\mu^+\nu_\mu$ to be $(3.49 \pm 0.46 \pm 0.27)\%$, where the first uncertainty is statistical and the second is systematic. The result is consistent with the value in PDG [22] within 2σ of uncertainty, but with improved precision. This study helps to extend our understanding on the decay mechanism of the Λ_c^+ SL decay. Based on this result and the previous BESIII work [14], we determine the ratio $\mathcal{B}(\Lambda_c^+ \rightarrow \Lambda\mu^+\nu_\mu)/\mathcal{B}(\Lambda_c^+ \rightarrow \Lambda e^+\nu_e) = 0.96 \pm 0.16 \pm 0.04$, which is compatible with unity. As the theoretical predictions on $\mathcal{B}(\Lambda_c^+ \rightarrow \Lambda\ell^+\nu_\ell)$ vary in a large range of 1.4% to 9.2% [2, 3, 4, 5, 6, 7, 8, 9, 10, 11, 12, 13], the measured $\mathcal{B}(\Lambda_c^+ \rightarrow \Lambda\mu^+\nu_\mu)$ in this work and $\mathcal{B}(\Lambda_c^+ \rightarrow \Lambda e^+\nu_e)$ in Ref. [14] provide stringent tests on these non-perturbative models.

5. Acknowledgments

The BESIII collaboration thanks the staff of BEPCII and the IHEP computing center for their strong support. This work is supported in part by National Key Basic Research Program of China under Contract No. 2015CB856700; National Natural Science Foundation of China (NSFC) under Contracts Nos. 11235005, 11235011, 11305090, 11322544, 11305180, 11335008, 11425524, 11505010; the Chinese Academy of Sciences (CAS) Large-Scale Scientific Facility Program; the CAS Center for Excellence in Particle Physics (CCEPP); the Collaborative Innovation Center for Particles and Interactions (CICPI); Joint Large-Scale Sci-

TABLE 2: Summary of the relative systematic uncertainties for $\mathcal{B}(\Lambda_c^+ \rightarrow \Lambda \mu^+ \nu_\mu)$.

Source	Uncertainty
μ^+ tracking	1.0%
μ^+ PID	2.0%
Λ reconstruction	2.5%
U_{miss} fit	1.5%
Peaking background $\Lambda_c^+ \rightarrow \Lambda \pi^+ \pi^0$	2.5%
$E_{\gamma\text{max}}$ requirement	2.6%
$M_{\Lambda\mu^+}$ requirement	2.0%
MC model	5.2%
$\mathcal{B}(\Lambda \rightarrow p \pi^-)$	0.8%
$N_{\Lambda_c^+}^{\text{tot}}$	1.0%
MC statistics	0.8%
Total	7.7%

tific Facility Funds of the NSFC and CAS under Contracts Nos. U1232201, U1332201; CAS under Contracts Nos. KJCX2-YW-N29, KJCX2-YW-N45; 100 Talents Program of CAS; National 1000 Talents Program of China; INPAC and Shanghai Key Laboratory for Particle Physics and Cosmology; German Research Foundation DFG under Contracts Nos. Collaborative Research Center CRC 1044, FOR 2359; Istituto Nazionale di Fisica Nucleare, Italy; Joint Large-Scale Scientific Facility Funds of the NSFC and CAS under Contract No. U1532257; Joint Large-Scale Scientific Facility Funds of the NSFC and CAS under Contract No. U1532258; Koninklijke Nederlandse Akademie van Wetenschappen (KNAW) under Contract No. 530-4CDP03; Ministry of Development of Turkey under Contract No. DPT2006K-120470; NSFC under Contract No. 11275266; The Swedish Research Council; U.S. Department of Energy under Contracts Nos. DE-FG02-05ER41374, DE-SC-0010504, DE-SC0012069, DESC0010118; U.S. National Science Foundation; University of Groningen (RuG) and the Helmholtzzentrum fuer Schwerionenforschung GmbH (GSI), Darmstadt; WCU Program of National Research Foundation of Korea under Contract No. R32-2008-000-10155-0. This paper is also supported by the Beijing municipal government under Contract Nos. KM201610017009, 2015000020124G064.

References

- [1] J. D. Richman and P. R. Burchat, *Rev. Mod. Phys.* **67**, 893 (1995); E. Eichten and B. Hill, *Phys. Lett. B* **234**, 511 (1990); M. Neubert, *Phys. Rep.* **245**, 259 (1994).
- [2] R. Pérez-Marcial *et al.*, *Phys. Rev. D* **40**, 2955 (1989).
- [3] M. Avila-Aoki *et al.*, *Phys. Rev. D* **40**, 2944 (1989).
- [4] F. Hussain *et al.*, *Z. Phys. C* **51**, 607 (1991).
- [5] G. V. Efimov *et al.*, *Z. Phys. C* **52**, 149 (1991).
- [6] Robert Singleton, *Phys. Rev. D* **43**, 2939 (1991).
- [7] A. Garcia and R. Huerta, *Phys. Rev. D* **45**, 3266 (1992).
- [8] H. Y. Cheng and B. Tseng, *Phys. Rev. D* **53**, 1457 (1995).
- [9] H. G. Dosch *et al.*, *Phys. Lett. B* **431**, 173 (1998).
- [10] R. S. Marques de Carvalho *et al.*, *Phys. Rev. D* **60**, 034009 (1999).
- [11] M. Pervin *et al.*, *Phys. Rev. C* **72**, 035201 (2005).
- [12] Y. L. Liu *et al.*, *Phys. Rev. D* **80**, 074011 (2009).
- [13] T. Gutsche *et al.*, *Phys. Rev. D* **93**, 034008 (2016).
- [14] M. Ablikim *et al.* [BESIII Collaboration], *Phys. Rev. Lett.* **115**, 221805 (2015).
- [15] M. Ablikim *et al.* [BESIII Collaboration], *Chin. Phys. C* **39**, 093001 (2015).
- [16] M. Ablikim *et al.* [BESIII Collaboration], *Nucl. Instrum. Meth. A* **614**, 345 (2010).
- [17] S. Agostinelli *et al.* [GEANT4 Collaboration], *Nucl. Instrum. Meth. A* **506**, 250 (2003).
- [18] S. Jadach, B. F. L. Ward and Z. Was, *Comput. Phys. Commun.* **130**, 260 (2000); *Phys. Rev. D* **63**, 113009 (2001).
- [19] D. J. Lange, *Nucl. Instrum. Meth. A* **462**, 152 (2001); R. G. Ping, *Chin. Phys. C* **32**, 599 (2008).
- [20] E. A. Kurav and V. S. Fadin, *Sov. J. Nucl. Phys.* **41**, 466 (1985).
- [21] E. Richter-Was, *Phys. Lett. B* **303**, 163 (1993); E. Barberio and Z. Was, *Comput. Phys. Commun.* **79**, 291 (1994).
- [22] K. A. Olive *et al.* [Particle Data Group], *Chin. Phys. C* **38**, 090001 (2014) and 2015 update.
- [23] J. C. Chen, G. S. Huang, X. R. Qi, D. H. Zhang, Y. S. Zhu, *Phys. Rev. D* **62**, 034003 (2000).
- [24] M. Ablikim *et al.* [BESIII Collaboration], *Phys. Rev. Lett.* **116**, 052001 (2016).
- [25] J. Y. Ge *et al.* [CLEO Collaboration], *Phys. Rev. D* **79**, 052010 (2009).
- [26] J. W. Hinson *et al.* [CLEO Collaboration], *Phys. Rev. Lett.* **94**, 191801 (2005).